IEEE Access
Multidisciplinary ⋮ Rapid Review ⋮ Open Access Journal

Received 14 July 2024, accepted 1 August 2024, date of publication 14 August 2024, date of current version 28 August 2024.

Digital Object Identifier 10.1109/ACCESS.2024.3443545

RESEARCH ARTICLE

Generation of Virtual Tunnels for Meal Activity Perception Assist With an Upper Limb Power Assist Exoskeleton Robot

YUE HOU, (Student Member, IEEE), AND KAZUO KIGUCHI, (Senior Member, IEEE)
Department of Mechanical Engineering, Kyushu University, Fukuoka 819-0395, Japan

Corresponding author: Kazuo Kiguchi (kiguchi@mech.kyushu-u.ac.jp)

This work involved human subjects or animals in its research. Approval of all ethical and experimental procedures and protocols was granted by the Research Ethics Committee of Kyushu University, School of Engineering, under Application No. 2023-01.

ABSTRACT Various human assistance robots that effectively assist the daily activities of persons with perception deficits have recently been developed. In this paper, a perception assist method with an upper limb power assist exoskeleton robot is proposed for meal activities, which are important in daily living. The proposed robot-based method assists users by appropriately assessing utensil trajectories and posture performance according to the target position of the user. A method to predict the user's target position based on the user's motion trajectories and shoulder muscle electromyographic (EMG) signals is also proposed. Two kinds of virtual tunnels (for the utensil trajectory and utensil posture) corresponding to the user's target position are defined in the proposed method to monitor the accuracy of the executed motion. The spatial relationship between the virtual tunnels is controlled to perform the eating task with the assistance of the power assist robot. The user's hand motion is automatically modified by the robot in real time if the utensil trajectory and/or posture exits the respective virtual tunnel during meal activities. The effectiveness of the proposed method is evaluated through experiments.

INDEX TERMS Virtual tunnels, exoskeleton robot, upper limb, perception assist, power assist, meal activity.

I. INTRODUCTION

In recent decades, population aging has become a serious issue worldwide [1]. Many types of power assist robots have been designed to help people with physical issues, such as elderly people or people with disabilities, with their daily activities [2], [3], [4], [5], [6], [7], [8]. In addition to declines in motor ability, many people with disabilities show cognitive decline due to illnesses or accidents. Moreover, overall neural degeneration may lead to sensory and perception deficits such as visual impairment and hearing loss in older people [9]. The degradation in sensory and perception abilities may lead to serious problems in the daily lives of elderly and disabled individuals. These individuals might not recognize the surrounding environment and perform tasks incorrectly. For instance, users walking in an area with obstacles may fall if they cannot accurately identify information such as the position and height of obstacles [10], [11], [12], [13], [14], [15]. To compensate for their deteriorated perceptual function, approaches that provide support can aid the user in perceiving the environmental information and correcting their inappropriate motions to properly complete tasks [10], [11], [12], [13], [14], [15], [16], [17], [18], [19], [20], [21], [22], [23], [24].

To date, many strategies, including predefined trajectory-based assistance techniques [25], [26], [27], [28], [29], intention-driven human-robot collaboration approaches [30], [31], [32], [33], [34], [35], [36] and perception assist methodologies [18], [19], [20], [21], [22], [23], [24], have been developed to leverage robots to aid users in performing different tasks with improved efficiency and precision. In predefined trajectory-based assistance methods, which are

The associate editor coordinating the review of this manuscript and approving it for publication was Venkata Rajesh Pamula.

© 2024 The Authors. This work is licensed under a Creative Commons Attribution-NonCommercial-NoDerivatives 4.0 License.
For more information, see https://creativecommons.org/licenses/by-nc-nd/4.0/

usually used in rehabilitation, the robot motion trajectory or motion pattern is designed in advance and not changed based on specific reactions or changes from the users [25], [26], [27], [28], [29]. These techniques are suitable for preset tasks with fixed trajectories but are not suitable for arbitrary tasks with variable trajectories in daily life movements. In intention-driven human-robot collaboration approaches, the robot should recognize the user's motion intentions and accordingly adjust its actions to better collaborate with the user, thereby completing the intended tasks [30], [31], [32], [33], [34], [35], [36]. These approaches focus on monitoring human movements and directing the robot to operate based on these observations, without considering whether these actions are appropriate for the tasks at hand or not. Therefore, these approaches can lead to inefficiencies in certain applications where human movements are not suitable for the intended task. On the other hand, perception assist methodologies focus on analyzing a user's movements and correct them if necessary. In these methods, the robot needs to infer a user's motion intention and provide automatic motion correction for inappropriate motions [18], [19], [20], [21], [22], [23], [24]. Therefore, when a power assist exoskeleton robot is used to help individuals with reduced cognitive ability perform daily activities, the robot can provide the necessary assistance required for these tasks. Since the user's hand movements may deviate from the appropriate trajectory during the movement process, the robot needs to offer necessary assistance to help users correct inappropriate motions while not hindering the user's normal movements via the perception assist methodology. This paper proposes a specific perception assist method for meal activities to assist individuals with declining perceptual functions who retain the fundamental perception abilities needed to perform reaching motions with the goal of obtaining food utilizing a utensil (forks, chopsticks, spoons, etc.) with the help of an upper limb power assist exoskeleton robot.

In perception assist approaches, it is important to obtain the user's motion intention in real time, which can be inferred by observing their body signals and their environmental interaction information [16], [17], [18], [19], [20], [21], [22], [23], [24], [30], [31], [32], [33], [34], [35], [36], [37], [38], [39], [40], [41], [42], [43], [44], [45], such as human biological signals (electromyography (EMG), electroencephalography (EEG), *etc*.), eye gaze, and motion characteristics (limb velocity/acceleration, motion trajectory, interaction force/torque with environments, etc.). To pick up food during meal activities, target position recognition is the main part of intention prediction [21], [22], [23]. Research has demonstrated that gaze cues and hand positions (trajectories) effectively predict the specific target position of a user's reaching motion [46]. However, when eye gaze is used for prediction, an additional measuring device is needed, and its accuracy is affected by lighting conditions and is limited if interference occurs [47]. When hand positions (trajectories) are used for prediction, some motions such as meal activities typically follow a curved path that can be inferred via feature points—the starting point of motions and the vertex of curved trajectories—to discern user intention [23]. However, recognizing these points, particularly the vertex along curved trajectories, suffers from delays exacerbated by sensor accuracy variances, often necessitating a threshold to confirm feature point locations after surpassing certain limits. Therefore, this study suggests the use of EMG signals to identify motion phases before and after the vertex, aiming for earlier detection of this point to increase target position estimation.

When the user's motion intention is recognized, it is also necessary to determine whether the user's motion is appropriate in the perception assist approach and to modify inappropriate motions as necessary [18], [19], [20], [21], [22], [23]. Threshold-based methods and machine learning approaches are applicable for detecting inappropriate motions of the user [18], [19], [20], [21], [22], [23], [48], [49], [50], [51], [52], [53], [54], [55]. A set of thresholds based on the user's joint angle/speed [49], [50] or end-effector motion spaces [18], [19], [20], [21], [22], [23], which can be called a ''virtual tunnel'' or ''virtual wall'', are defined as the boundary of an acceptable motion range. When the human body moves beyond/into the boundary, the motion is considered inappropriate [18], [19], [20], [21], [22], [23], [49], [50], [51], [52], [53]. Machine learning approaches such as neural networks [54] and support vector machines (SVMs) [55] can also be used to recognize and classify appropriate and inappropriate motions. In previous research, motion trajectory evaluation and modification have been performed with such approaches [18], [19], [20], [21], [22], [23], [49], [50], [51], [52], [53]. Although not only the user's motion trajectory and utensil's posture but also their corporative relation are important in the context of meal activities, their corporative relation has not been discussed in the existing methods.

In this paper, to infer a user's motion intention more accurately during meal activities and address the challenge of linked control of both the utensil trajectory and posture, a meal activity perception assist method is proposed to enable users to obtain food from the chosen dish with a utensil following a suitable trajectory and posture. The proposed method can be divided into two parts. First, since the user's motion intention is acquired by estimating the target position, the method involves determining the target position by tracking the applied utensil trajectory and monitoring the EMG signals of the shoulder muscles. Shoulder EMG signals are used to identify different motion phases in real time, and the feature point (vertex) in the motion trajectory are accurately obtained to improve the target position prediction accuracy. Furthermore, the spatial relationship between two kinds of virtual tunnels (one for the utensil trajectory and one for the utensil posture) is defined to aid users in maintaining the utensil trajectory and utensil posture within acceptable ranges and accurately performing the intended task. The two virtual tunnels are interrelated and can facilitate coordinated control

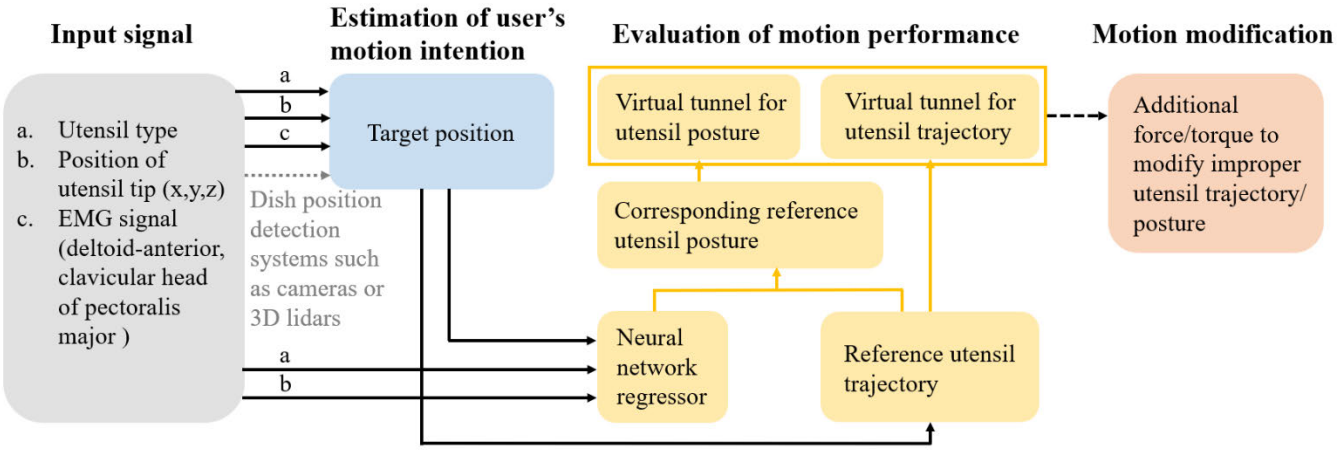

FIGURE 1. Proposed perception assist method for meal activities.

of the utensil trajectory and utensil posture. The effectiveness of the proposed method for meal activities is confirmed through experiments in which an exoskeleton upper limb power assist robot is used.

II. MEAL ACTIVITIES PERCEPTION ASSIST WITH AN UPPER LIMB POWER ASSIST EXOSKELETON ROBOT

A meal activity perception assist method is proposed to aid individuals with perception impairments in properly performing the motion of reaching for food while using a utensil, with the help of an upper limb power assist exoskeleton robot. The proposed method consists of two parts. In the first part, the user's motion intention is estimated, specifically by predicting from which dish the user intends to retrieve food. In the second part, inappropriate utensil trajectories and utensil postures are detected and modified, enabling the user to complete the expected motion of obtaining food. The overall flowchart of the proposed method is shown in Fig. 1.

A. ESTIMATION OF THE USER'S TARGET POSITION

Using the motion trajectory of the upper limb end-effector (hand/utensil) is a practical method to estimate the position of the user's intended dish. Specifically, in daily activities, when healthy individuals use utensils to obtain food, the trajectory of the hand/utensil typically begins at the table and moves to a certain height before moving down to the intended dish to retrieve food (refer to Fig. 2(a)). It is considered the characteristics of the task tend to generate consistent motion patterns. Based on this context, three pivotal trajectory points (initial position $\boldsymbol{P_h}$, intermediate position $\boldsymbol{P_p}$ and target position $\boldsymbol{P_o}$) are defined in this study to delineate the characteristics of the curved utensil trajectory. These three points are defined as the position of the utensil tip before the motion starts, the vertex of the utensil trajectory, and the location of the dish from which the user wants to retrieve food. By analyzing motion data acquired from healthy individuals, the correlation among the coordinates of these three points can

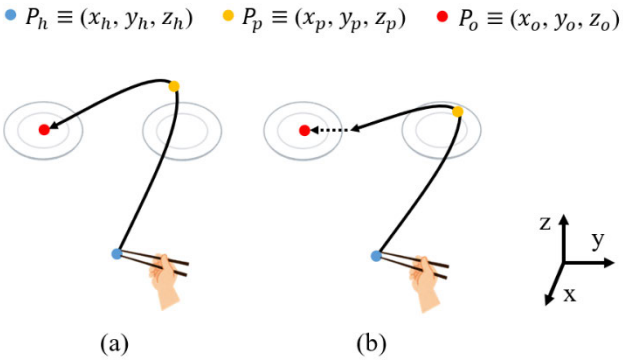

FIGURE 2. Utensil trajectories during meal activities in daily life. Point P_h is the initial position of the utensil tip before the motion starts; P_p is the trajectory's vertex, signifying the intermediate position in the motion process; and P_o is the location of the intended dish, denoting the user's target position. (a) Appropriate utensil trajectory. (b) Inappropriate utensil trajectory.

be established. As demonstrated in our previous study [23], given the coordinates of the initial and intermediate positions, the user's target position can be estimated. The initial position is the location where the motion begins and can be directly observed. Timely and precise acquisition of the intermediate position allows for the estimation of the user's target position. Nonetheless, for individuals with perception impairments, the prediction of the target position based solely on the initial and intermediate positions may lead to inconsistencies, as illustrated in Fig. 2(b). By utilizing data acquired from dish position detection systems such as cameras or 3D lidars [21], [22], the positioning of all the dishes can be precisely determined. With this technology, the dish closest to the predicted position can be determined as the target position.

The movement of utilizing a utensil to pick up food involves coordinated action of the forearm, elbow, and shoulder joints [56]. Given the activity in these regions, EMG signals from the associated muscles can serve as indirect indicators of the user's motion trajectory. As the user transitions from the initial position to the intermediate position,

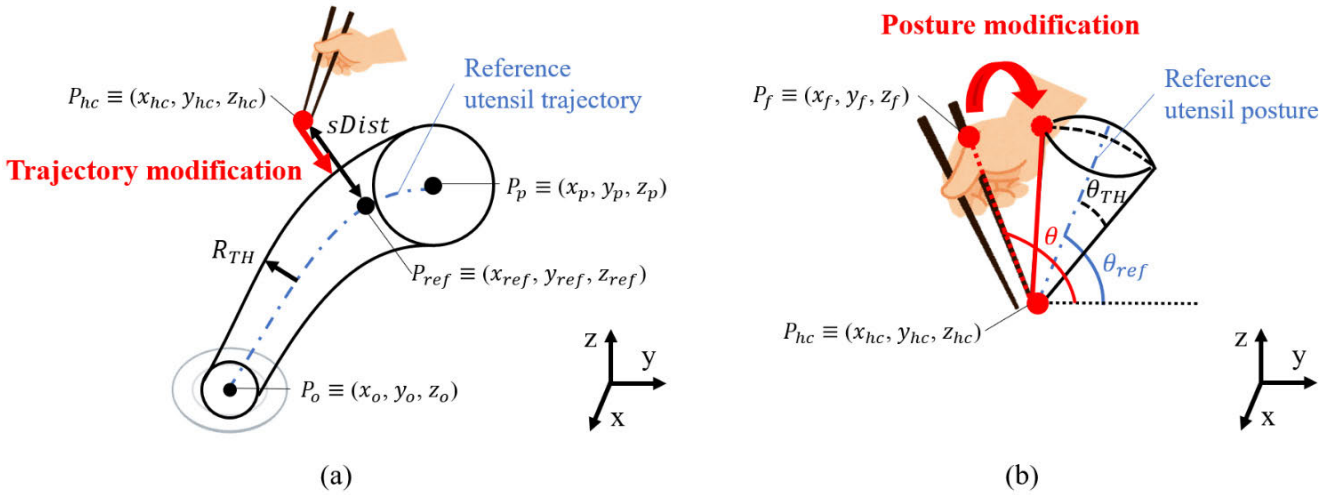

FIGURE 3. Modification of the trajectory and posture using virtual tunnels. (a) Modification of an inappropriate utensil trajectory with a virtual tunnel. Point P_p is the intermediate position and P_o is the target position, as previously defined. P_{hc} is the location of the utensil tip. P_{ref} indicates the nearest point in the reference trajectory to P_{hc}. R_{TH} represents the radius of the virtual tunnel. (b) Modification of an inappropriate utensil posture with a virtual tunnel. The utensil posture depends on the position of the utensil tip P_{hc}, with respect to P_f, the position of the base of the index finger. θ represents the observed utensil posture. θ_{ref} is the reference utensil posture. The tolerance angle θ_{TH} represents the size of the virtual tunnel.

the shoulder flexion angle increases, which corresponds to an increase in the intensity of the EMG signals of the involved muscles. As the user subsequently moves from the intermediate position to the target position, the shoulder flexion angle begins to decrease. This reduction in flexion is associated with a corresponding decrease in the EMG signal intensity of the involved muscles. Therefore, as the shoulder flexion angle increases or decreases during movement, the EMG signals related to the shoulder joint flexion angle change, reflecting the transition in the movement pattern. This information can be used to infer the arrival time at the intermediate position, which is crucial for tracking the motion progress. The deltoid-anterior and pectoralis major (clavicular head) muscles, which serve as agonists for shoulder flexion, exhibit significant activity during this movement [57], [58], [59]. Therefore, the EMG signals of these two muscles are used to determine the exact moment at which a user reaches the intermediate position in motion. When an exoskeleton robot is utilized, the position of the utensil's tip is calculated via the exoskeleton kinematics in real time, which determines the hand's position based on the exoskeleton's link lengths and joint angles, extending the kinematic chain to incorporate the utensil's fixed relationship with the hand during movement. This method integrates shoulder EMG information with mathematical relationships among key trajectory points, including initial, intermediate, and target positions [23]. By enhancing the precision of identifying the intermediate position, it improves the accuracy of predicting the user's intended target position.

B. MOTION EVALUATION AND MODIFICATION

Once the target position has been determined, to enable the user to complete the intended meal task, it is necessary to evaluate whether the user's motion is performed properly by monitoring the trajectory and posture of the utensil held by the user in real time. In the proposed method, two virtual tunnels (one for the tip trajectory and the other for the posture) are defined to assess the utensil trajectory and posture performance. When the user's utensil trajectory and posture remain within the virtual tunnels, they are recognized as appropriate. However, when they deviate from this range, they are deemed inappropriate. The integration of these two virtual tunnels enables coordinated control of the utensil trajectory and posture. When the user performs inappropriate motions, deviations occur as utensil trajectories/postures exceed the boundaries of the virtual tunnel, and the power assist exoskeleton robot applies modification forces/torques to guide the utensil trajectory/posture back within the virtual tunnels. The proposed method continuously evaluates the appropriateness of user movements, from the initial prediction of the target position through to its successful attainment.

1) VIRTUAL TUNNEL FOR UTENSIL TRAJECTORY

The definition of the virtual tunnel for the utensil trajectory is shown in Fig. 3(a). After the user's trajectory arrives at the intermediate position and the target position is estimated, a reference trajectory toward the intended dish is calculated. The reference utensil trajectory approximates a quadratic curve passing through the intermediate position $\boldsymbol{P_p}$ and target position $\boldsymbol{P_o}$. Relative to the x-axis, this trajectory can be described by the following equations:

$$y = \frac{y_o - y_p}{(x_o - x_p)^2}(x - x_p)^2 + y_p \tag{1}$$

$$z = \frac{z_o - z_p}{(x_o - x_p)^2}(x - x_p)^2 + z_p \tag{2}$$

Around this trajectory, a virtual tunnel of radius $\boldsymbol{R_{TH}}$ is generated. Initially, the tunnel width offers a generous movement range, reducing the need to have a precise trajectory, thereby reducing user strain. However, as the user approaches the target position, the tunnel width decreases, helping users precisely pick up food. Assume that the maximum and minimum radii of the virtual tunnel are $\boldsymbol{R_{TH,max}}$ and $\boldsymbol{R_{TH,min}}$, respectively. As the user approaches the target position, the radius of the virtual tunnel progressively decreases. The formula to achieve this functionality, represented by $\boldsymbol{R_{TH}}$, is provided below:

$$\boldsymbol{D_{hc,o}} = \sqrt{(x_{hc} - x_o)^2 + (y_{hc} - y_o)^2 + (z_{hc} - z_o)^2} \quad (3)$$

$$\boldsymbol{D_{p,o}} = \sqrt{(x_p - x_o)^2 + (y_p - y_o)^2 + (z_p - z_o)^2} \quad (4)$$

$$\boldsymbol{R_{TH}} = (\boldsymbol{R_{TH,max}} - \boldsymbol{R_{TH,min}}) \left(\frac{\boldsymbol{D_{hc,o}}}{\boldsymbol{D_{p,o}}}\right)^2 + \boldsymbol{R_{TH,min}} \quad (5)$$

where $\boldsymbol{D_{hc,o}}$ denotes the Euclidean distance between the utensil tip $\boldsymbol{P_{hc}}$ and the target position $\boldsymbol{P_o}$. Similarly, $\boldsymbol{D_{p,o}}$ represents the Euclidean distance between the intermediate position $\boldsymbol{P_p}$ and the target position $\boldsymbol{P_o}$. Although the radius of the virtual tunnel near the target position should be minimized, it is essential to consider elements such as typical dish sizes to ensure that the radius $\boldsymbol{R_{TH,min}}$ remains large enough for users to complete eating tasks. In the initial phase, the radius $\boldsymbol{R_{TH,max}}$ should be set to accommodate more user behaviors.

If the utensil's tip strays outside this tunnel, namely, if the spatial geometric distance ***sDist*** surpasses the threshold $\boldsymbol{R_{TH}}$, a modification force in the direction of ***sDist*** is applied to redirect the utensil tip. The formula for calculating ***sDist*** is described as follows:

$$\boldsymbol{sDist} = \sqrt{(x_{hc} - x_{ref})^2 + (y_{hc} - y_{ref})^2 + (z_{hc} - z_{ref})^2} \quad (6)$$

where $\boldsymbol{P_{hc}} \equiv (x_{hc}, y_{hc}, z_{hc})$ is the position of the utensil tip and where $\boldsymbol{P_{ref}} \equiv (x_{ref}, y_{ref}, z_{ref})$ denotes the nearest point on the reference utensil trajectory to $\boldsymbol{P_{hc}}$, indicating the ideal position of the utensil tip. To refine this distance in three-dimensional space, constraints are set for the x, y, and z directions based on the tunnel radius. The appropriateness of the trajectories executed by the user in the x-, y-, and z-axis directions is determined via Eqs. (7), (8) and (9):

$$\boldsymbol{sDist_x} = |x_{hc} - x_{ref}| > \sqrt{\frac{R_{TH}^2}{3}} \quad (7)$$

$$\boldsymbol{sDist_y} = |y_{hc} - y_{ref}| > \sqrt{\frac{R_{TH}^2}{3}} \quad (8)$$

$$\boldsymbol{sDist_z} = |z_{hc} - z_{ref}| > \sqrt{\frac{R_{TH}^2}{3}} \quad (9)$$

These formulas are used to determine the directions in which the motion modification forces should be applied.

2) VIRTUAL TUNNEL FOR UTENSIL POSTURE

To evaluate and modify inappropriate utensil postures, a second virtual tunnel was created, as shown in Fig. 3(b). The utensil posture is determined by the position of its tip $\boldsymbol{P_{hc}}$ in relation to the base of the index finger $\boldsymbol{P_f}$. The postures in the x-y, z-x, and z-y planes are defined via Eqs. (10), (11), and (12):

$$\boldsymbol{\theta_{xy}} = \mathbf{atan2}(x_{hc} - x_f, y_{hc} - y_f) \quad (10)$$

$$\boldsymbol{\theta_{zx}} = \mathbf{atan2}(z_{hc} - z_f, x_{hc} - x_f) \quad (11)$$

$$\boldsymbol{\theta_{zy}} = \mathbf{atan2}(z_{hc} - z_f, y_{hc} - y_f) \quad (12)$$

Here, $\boldsymbol{\theta}$ represents the user-induced utensil posture, while $\boldsymbol{\theta_{ref}}$ represents the reference posture. A virtual tunnel characterized by a tolerance angle $\boldsymbol{\theta_{TH}}$ is established surrounding the reference posture. The maximum and minimum sizes of the virtual tunnel are assumed to be $\boldsymbol{\theta_{TH,max}}$ and $\boldsymbol{\theta_{TH,min}}$, respectively. Analogous to trajectory modification, this posture virtual tunnel is designed to narrow progressively as the user approaches the target position. The formula for calculating $\boldsymbol{\theta_{TH}}$ is presented below to accomplish this function:

$$\boldsymbol{\theta_{TH}} = (\boldsymbol{\theta_{TH,max}} - \boldsymbol{\theta_{TH,min}}) \left(\frac{\boldsymbol{D_{hc,o}}}{\boldsymbol{D_{p,o}}}\right)^2 + \boldsymbol{\theta_{TH,min}} \quad (13)$$

As illustrated in Eqs. (3) and (4), $\boldsymbol{D_{hc,o}}$ is the distance from the utensil tip $\boldsymbol{P_{hc}}$ to the target position $\boldsymbol{P_o}$, and $\boldsymbol{D_{p,o}}$ is the distance from the intermediate position $\boldsymbol{P_p}$ to $\boldsymbol{P_o}$. For the posture virtual tunnel, the minimum size $\boldsymbol{\theta_{TH,min}}$ should consider the natural tilt range of general human hand operations during meal activities, thereby ensuring the basic freedom of the utensil posture. Additionally, $\boldsymbol{\theta_{TH,max}}$ needs to enhance the initial posture flexibility.

To quickly detect notable deviations in any direction and apply the necessary corrective torque, trigger angles—defined as $\boldsymbol{\theta_{TH,xy}}$, $\boldsymbol{\theta_{TH,zx}}$ and $\boldsymbol{\theta_{TH,zy}}$—are set in the x-y, z-x, and z-y planes, all of which are constrained to not surpass $\boldsymbol{\theta_{TH}}$. If the utensil posture exceeds the tolerance limits along any of the axes, a corresponding modification torque is needed. The criteria to identify unsuitable postures are given by Eqs. (14), (15), and (16):

$$\boldsymbol{\theta_{gap,xy}} = |\boldsymbol{\theta_{xy}} - \boldsymbol{\theta_{ref,xy}}| > \boldsymbol{\theta_{TH,xy}} \quad (14)$$

$$\boldsymbol{\theta_{gap,zx}} = |\boldsymbol{\theta_{zx}} - \boldsymbol{\theta_{ref,zx}}| > \boldsymbol{\theta_{TH,zx}} \quad (15)$$

$$\boldsymbol{\theta_{gap,zy}} = |\boldsymbol{\theta_{zy}} - \boldsymbol{\theta_{ref,zy}}| > \boldsymbol{\theta_{TH,zy}} \quad (16)$$

Here, $\boldsymbol{\theta_{gap}}$ represents the absolute difference between the observed utensil posture $\boldsymbol{\theta}$ and the reference posture $\boldsymbol{\theta_{ref}}$. By using these equations, the direction of the unsuitable utensil posture can be determined, guiding the application of the modification torque.

3) TRAJECTORY/POSTURE MODIFICATION USING ADDITIONAL MODIFICATION FORCE/TORQUE

When implementing these adjustments, it is crucial to balance user comfort with efficient trajectory and posture modifications. Abrupt changes in the forces/torques at virtual tunnel

boundaries can make the user experience feel disjointed or unnatural. To address this issue, an external boundary is delineated around the virtual tunnels. Unlike conventional methods that apply constant modification forces/torques, the system's modification forces/torques gradually change between the tunnel boundary and the external boundary. The external boundary is defined around the virtual tunnels. The size of this external boundary is influenced by parameters ΔL_1 and ΔL_2, which are positioned at distances of $\Delta L_1 \times R_{TH}$ and $\Delta L_2 \times \theta_{TH}$ from the tunnel boundary, respectively. Within the confines of the virtual tunnel, no modifications are applied. These modifications are applied only when the utensil trajectory or posture surpasses the tunnel boundaries. In the space between the tunnel boundary and the external boundary, the force or torque applied for modification incrementally changes depending on either $sDist$ or θ_{gap}, thus manifesting a linear progression from 0 to the maximum value. If $sDist$ or θ_{gap} exceeds the external boundary, the full modification force/torque is applied.

During trajectory corrections, the magnitude of the modification force, $F(sDist)$, depends on the overall deviation of the utensil from its reference trajectory in space. The expression for this force is detailed in the following formula:

$$F(sDist) = \begin{cases} 0, & sDist \leq R_{TH} \\ K_f F_{max}, & R_{TH} < sDist < (1+\Delta L_1) * R_{TH} \\ F_{max}, & sDist \geq (1+\Delta L_1) * R_{TH} \end{cases} \quad (17)$$

$$K_f = \frac{(sDist - R_{TH})}{\Delta L_1 * R_{TH}} \quad (18)$$

When $sDist$ exceeds the boundaries of the virtual tunnel and deviations in certain directions surpass their set constraints, a modification force is proportionally applied to those specific directions based on the deviation's magnitude. In posture adjustments, the modification torque $T(\theta_{gap})$ is considered separately for the x-y, z-x, and z-y directions. In this process, three torques corresponding to the posture deviation angle are calculated in the $\theta_{gap,xy}$, $\theta_{gap,zx}$, and $\theta_{gap,zy}$ directions. These are subsequently integrated to modify the utensil posture comprehensively. The following formula defines the modification torque applied in each direction:

$$T(\theta_{gap}) = \begin{cases} 0, & \theta_{gap} \leq \theta_{TH} \\ K_t T_{max}, & \theta_{TH} < \theta_{gap} < (1+\Delta L_2) * \theta_{TH} \\ T_{max}, & \theta_{gap} \geq (1+\Delta L_2) * \theta_{TH} \end{cases} \quad (19)$$

$$K_t = \frac{(\theta_{gap} - \theta_{TH})}{\Delta L_2 * \theta_{TH}} \quad (20)$$

4) INTEGRATION OF THE TWO VIRTUAL TUNNELS

To understand and modify the utensil trajectory and posture simultaneously and coordinately, the two virtual tunnels must be linked in space (Fig. 4). As the user guides their hand

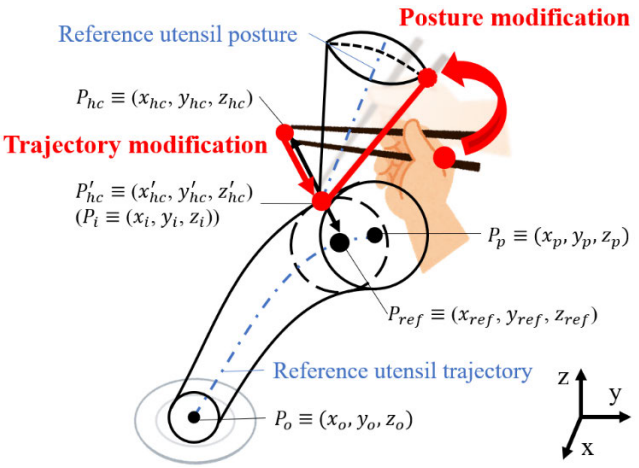

FIGURE 4. Integration of two virtual tunnels. $P_{hc}{}'$ is the expected position of the utensil tip. Under the circumstances in this figure, the expected position of the utensil tip is also the intersection (P_i) of the perpendicular line from P_{hc} to the reference trajectory and the virtual tunnel for trajectory.

toward the desired location, the posture of the utensil changes with movement. This ensures that the utensil has the optimal posture for food retrieval. Therefore, the key to linking these two virtual tunnels is to determine the spatial relationship between the utensil trajectory and posture. Regression neural networks, which are popular machine learning models, can be used to determine relationships between input and output datasets. Consequently, these trained models can be utilized for prediction. In our research, a neural network regressor was employed to connect the reference utensil trajectory and posture. By using motion data from healthy participants, the reference utensil posture θ_{ref} based on the reference utensil position P_{ref} can be predicted in real time. This is crucial as P_{ref} provides a stable benchmark, especially when the actual utensil position deviates from the determined virtual tunnel.

Following the construction of the virtual tunnel for the utensil trajectory, the virtual tunnel for the utensil posture is dynamically synthesized. The anticipated utensil tip position P'_{hc} serves as the focal point, which is based on the reference utensil posture θ_{ref}. P'_{hc} is determined via the spatial geometric distance $sDist$ and real-time utensil position P_{hc}, as depicted in Eq. (21):

$$P'_{hc} = \begin{cases} P_{hc}, & sDist < R_{TH} \\ P_i, & sDist \geq R_{TH} \end{cases} \quad (21)$$

Here, P_i denotes the intersection point of the perpendicular from P_{hc} to the reference trajectory and the boundary of the trajectory virtual tunnel. Specifically, if the utensil tip remains within the trajectory virtual tunnel, its corresponding posture tunnel is designed using the current position of the utensil tip P_{hc} as the focal point. However, if the utensil tip drifts outside this tunnel, the focal point of the relevant posture tunnel is shifted to the adjusted position of the utensil tip P_i. Therefore, the two virtual tunnels intersect via a perpendicular line, as determined by the focal point of the posture tunnel and

orthogonal to the trajectory tunnel's central line (reference utensil trajectory). This approach enables simultaneous and coordinated control over the user's utensil trajectory and posture.

III. EXPERIMENTS

A. EXPERIMENTAL AIM

To demonstrate the efficacy of the proposed perception-assist method for meal activities, two kinds of experiments were conducted. Experiment-1 was carried out for two purposes: first, to confirm that the EMG signals of the deltoid-anterior and pectoralis major (clavicular head) muscles can be used to determine if a user's movement has reached the intermediate position and evaluate the ability to accurately predict the user's target position; second, to demonstrate the feasibility of utilizing neural network models to establish the correlation between the utensil trajectory and the utensil posture throughout the movement process. Experiment-2 aimed to demonstrate the efficacy of the defined virtual tunnels in correcting users who performed inappropriate utensil trajectories/postures by wearing a power assist exoskeleton robot in practical settings. This experiment aims to demonstrate the practical applicability of the proposed methods. The experiments were approved by the research ethics committee of Kyushu University, School of Engineering (2023-01). After being fully briefed on the experiments, the participants provided their informed consent.

B. EXPERIMENTAL SETUP AND PROCEDURE

1) EXPERIMENT-1

In this experiment, three healthy right-handed participants (one male subject and two female subjects) participated. Table 1 lists participant data on age, sex, height, weight, and hand dominance. The participants performed motions that simulated reaching for food using utensils in real-life scenarios, interacting with designated positional markers rather than tangible dishes in the process. The experiment was confined within a 300 mm × 300 mm workspace on a desktop and partitioned into nine equally sized regions arranged in a 3×3 grid pattern, as shown in Fig. 5(a). Each region, measuring 100 mm × 100 mm, corresponded to a specific target position index. Positional markers were placed at the center of each region to indicate the target positions. The experiment involved the use of three kinds of utensils: a fork, chopsticks, and a spoon. The utensil trajectories and postures for different target positions and the corresponding user's EMG signals were recorded. To measure the utensil trajectory and posture, markers were attached to both the utensil tip and the base of the participant's index finger, and a motion tracker (V120 Duo, OptiTrack) was utilized to measure the marked positions, capturing data at 120 frames per second (fps). Furthermore, EMG sensors (EM-U810BF, Ultium) were used to measure the EMG signals (Table 2) of each participant's shoulder muscles. EMG sensors were positioned along the muscle fibers at the belly of the selected muscle, ensuring placement at the most prominent part during

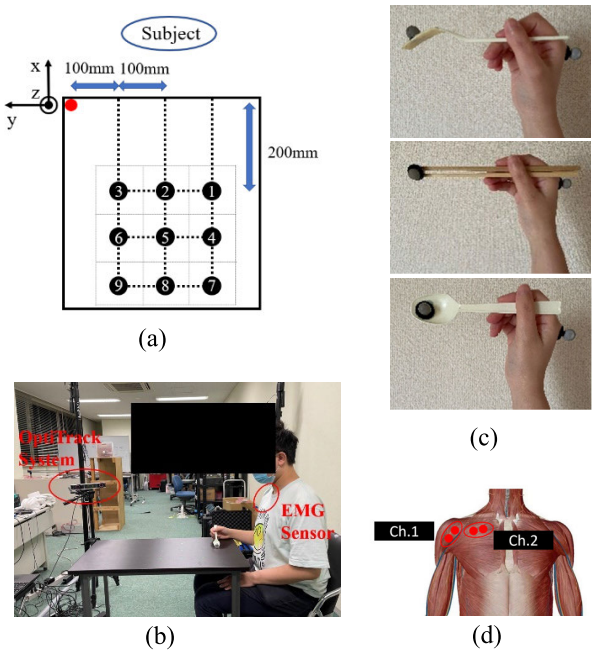

FIGURE 5. Experimental setup. (a) Settings for the marks on the desktop. (b) The scenario in which the experiment was conducted. (c) The utensils that were utilized. (d) Attachment locations of EMG sensors on shoulder muscles.

resistance contraction (see Fig. 5(d)). The EMG data were recorded at a sampling rate of 2 kHz, with the low-pass filter set at 500 Hz and the high-pass filter set at 10 Hz. Additionally, synchronization signals were established between the data collected by the OptiTrack system and the EMG signals. During this experiment, the participants sat straight so that their upper body posture was not altered. The experimental procedure can be described as follows.

1. Each participant was instructed to hold the fork at the initial position on the table; then, the fork trajectory, fork posture, and subject's EMG signals were recorded.
2. The participant starts to perform a reaching motion toward target position 1 and then returns to the initial position. The participant repeats this process by performing motions toward target positions 2 to 9 in order.
3. Steps 1 and 2 are repeated three times.
4. The fork was replaced with chopsticks and then a spoon, and steps 1 to 3 were repeated.

In this experiment, a ten-second break was provided between each motion trial to ensure participant recovery. Prior to data collection for each motion trial, the motion tracking system underwent consistency checks. Additionally, the EMG signals were monitored to remain near zero under static conditions, thus establishing a stable baseline.

2) EXPERIMENT-2

In this experiment, a healthy right-handed female participant, aged 29 years, with a height of 160 cm and a weight of 50 kg, was included. The upper limb power assist exoskeleton robot used for the experiment is shown in Fig. 6 and was attached to a wheelchair. This robot employs an EMG-based control

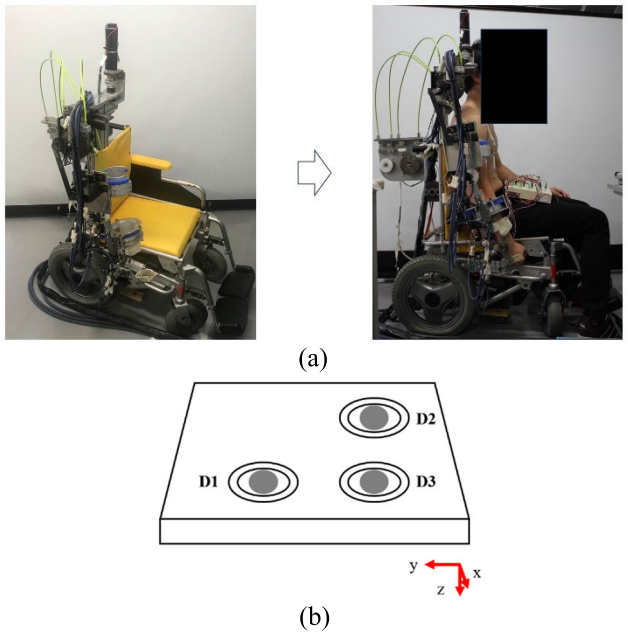

FIGURE 6. (a) Overview of the 7DOF upper limb power assist exoskeleton robot. (b) Experimental environment.

TABLE 1. Participant details.

Participant	Age	Sex	Height (cm)	Weight (kg)	Hand dominance
1	31	Female	165	50	Right
2	29	Male	174	71	Right
3	28	Female	162	51	Right

TABLE 2. Muscles for each EMG channel.

EMG Channel (Ch)	Muscle
Ch. 1	Deltoid-anterior
Ch. 2	Pectoralis major (clavicular head)

strategy to respond to the participant's motion [4], while the perception assist method proposed in this study allows the robot to adjust the participant's inappropriate motions by applying modification forces or torques. The robot supports seven degrees of freedom (7DOF) for upper limb movements, including multiple motions of the shoulder, elbow, forearm, and wrist. Two degrees of freedom for the shoulder and elbow are enabled by wired DC motors, while the other joints are directly controlled via DC motors. The angle of each joint is measured by encoders, and the robot's forearm and wrist are equipped with tri-axial force sensors to measure the interaction forces with the user. For the experimental setup, the participant performed tasks while wearing the exoskeleton robot in the environment depicted in Fig. 6(b). This environment consists of three dishes labeled D1, D2, and D3, whose positions are predefined at coordinates (-0.50 m, 0.20 m, 0.50 m), (-0.60 m, 0.10 m, 0.50 m), and (-0.50 m, 0.10 m, 0.50 m), respectively, in the robot's world coordinate system. These positions are assumed to be measured practically with a dish position detection system, although these position data are directly used in this study. The participant was instructed to select one dish as a target and use a utensil to retrieve food from the chosen dish.

To assess the effectiveness of the proposed perception assist method, the participant was instructed to execute the motion using inappropriate utensil trajectories and/or postures. The experiment was divided into three trials: in trial A, the participant deliberately performed an inappropriate utensil trajectory during motion, deviating slightly from the planned path and exceeding the boundaries of the virtual tunnel, while the utensil posture remained within the normal operational range. In trial B, the user moved the utensil normally toward the chosen dish, but the utensil posture was intentionally altered during the motion, deviating from the planned posture and exceeding the boundaries of the virtual tunnel. In trial C, which was a combination of the strategies applied in trials A and B, incorrect utensil trajectories and postures were both applied during motion.

The experimental procedure was set as follows.

1. The participant was instructed to pick up a utensil and place it at the initial position on the table.
2. The participant conducted Trial A.
3. Step 1 was repeated, and the participant conducted Trial B.
4. Step 1 was repeated, and the participant conducted Trial C.

Empirically, the trajectory virtual tunnel is defined with a minimum radius $\boldsymbol{R_{TH,min}}$ of 50 mm and an upper limit $\boldsymbol{R_{TH,max}}$ capped at 100 mm. In terms of the posture virtual tunnel, tolerance angles are set with a minimum size $\boldsymbol{\theta_{TH,min}}$ at 15 degrees and a maximum $\boldsymbol{\theta_{TH,max}}$ of 30 degrees. The maximum motion modification force, denoted as $\boldsymbol{F_{max}}$, was determined to be 1.4 N [60], while the posture modification torque, $\boldsymbol{T_{max}}$, was set at 2.5 N/m. The external boundaries of the virtual tunnels lie at 1.2 times $\boldsymbol{R_{TH}/\theta_{TH}}$ from the reference trajectory/posture, with $\boldsymbol{\Delta L_1}$ and $\boldsymbol{\Delta L_2}$ both being 0.2.

IV. RESULTS AND DISCUSSION

A. EXPERIMENT-1

As a representative result, Fig. 7 shows the measured utensil trajectory and processed EMG signals of the deltoid-anterior muscle and pectoralis major muscle (clavicular head), when participant 1 performed the motion of acquiring food from target position 9 using a fork. Fig. 7(a) shows the EMG results for the deltoid-anterior and pectoralis major (clavicular head) muscles. During preprocessing, the raw EMG signals were processed by taking the root mean square (RMS) over a 500 ms window length to extract features from the original EMG signals. A median filter was subsequently used to remove noise and smooth the EMG-RMS signals over a 15 ms window size. The filtered EMG-RMS signals

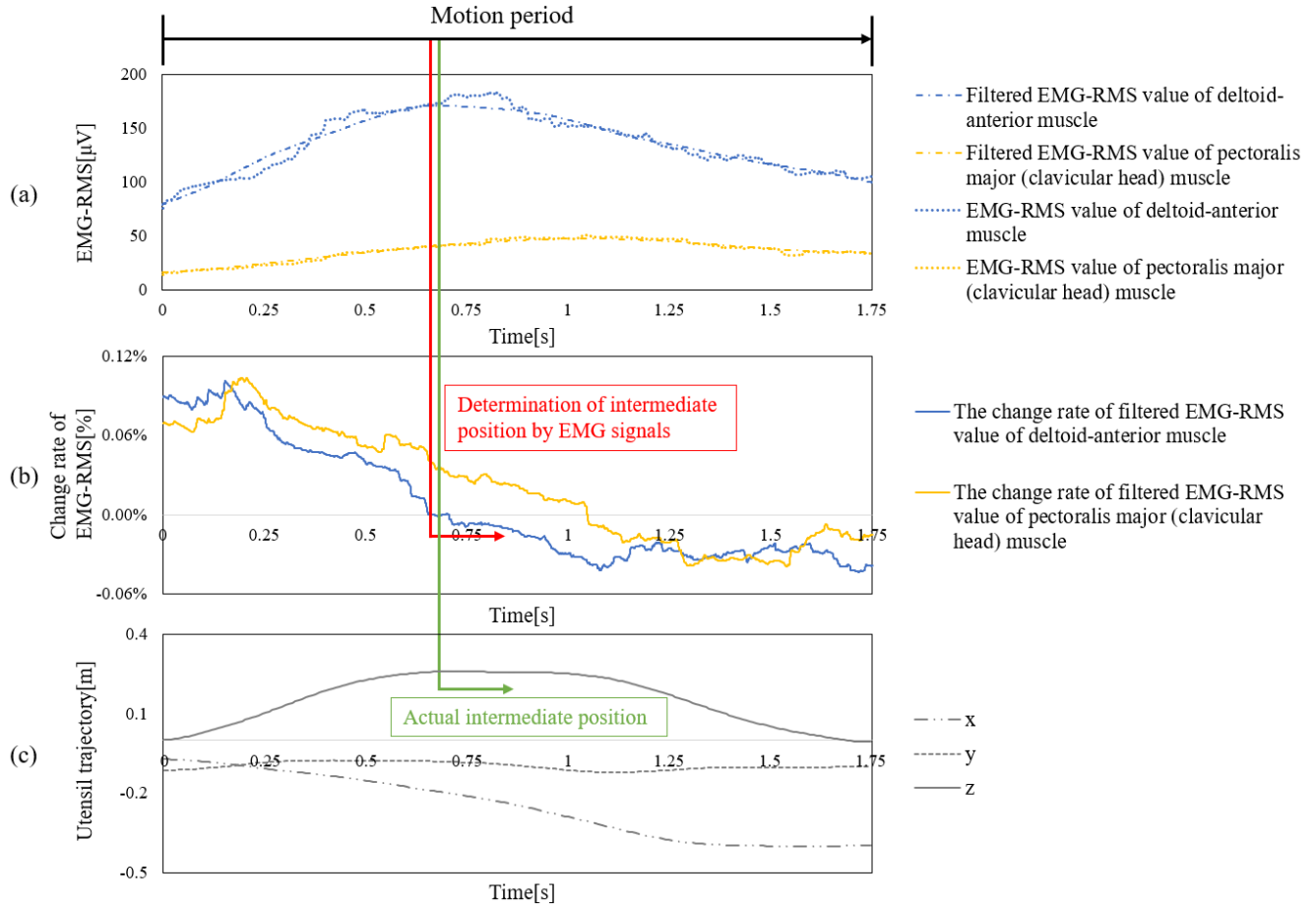

FIGURE 7. Example result of the estimation of intermediate position based on the EMG signals for subject 1 using a fork moving toward target position nine. (a) The EMG-RMS values of the deltoid-anterior and pectoralis major (clavicular head) muscles were calculated with a 500 ms window length and filtered using a median filter with a window size of 15 ms. (b) The change rate of the filtered EMG-RMS values of the deltoid-anterior and pectoralis major (clavicular head) muscles. (c) The measured utensil trajectory.

are represented by the dashed-dotted line. During movement from the initial position to the intermediate position, the RMS signals of both muscles increased with the flexion of the shoulder. Conversely, in the trajectory from the start to the target position, the RMS signals of both muscles decreased with the extension of the shoulder. Fig. 7(b) shows the rate of change in the EMG-RMS signals for the deltoid-anterior and pectoralis major (clavicular head) muscles. Fig. 7(b) shows that the EMG-RMS signal peaks at the instant when the EMG-RMS rate of change transitions from positive to negative. Fig. 7(c) presents the measured utensil trajectory. The red arrow indicates the moment at which the trajectory reaches the intermediate position, as predicted by the EMG signal, while the green arrow indicates the actual intermediate position along the utensil trajectory. The deviations between the actual intermediate position reached by the user's utensil trajectory and the location estimated at that moment via the EMG signals in the x and y directions are detailed in Fig. 8.

In a previous study [23], the target position, represented by the coordinates (x_o, y_o) of a given utensil, was derived from the intermediate position P_p and the initial position P_h. The

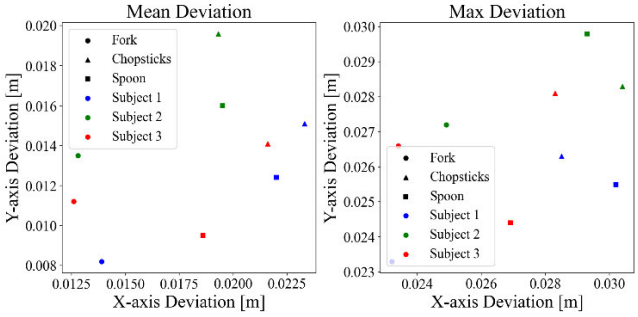

FIGURE 8. The deviation in the distances on the x and y axes between the intermediate positions reached by the users' utensil trajectories and the positions at those moments estimated through EMG signals in Experiment-1.

relationships are captured in the following equations:

$$x_o = a_{utensil,x} * x_p + b_{utensil,x} * x_h + c_{utensil,x} \quad (22)$$

$$y_o = a_{utensil,y} * y_p + b_{utensil,y} * y_h + c_{utensil,y} \quad (23)$$

The z-coordinate for the target position is not included because motion targets lie on the table, making the

z-coordinate constant. The coefficients a, b, and c are adjusted on the basis of the utensil and the x or y axis. By inputting the EMG-predicted intermediate position into the target position calculation formula, and applying coefficients specifically derived from this study, the error between the actual target position and the estimated target position was computed. Based on the data acquired across all movement trials, the most significant deviation between the inferred and actual intermediate positions was 0.0304 m on the x-axis and 0.0298 m on the y-axis. The inferred and actual intermediate positions were both incorporated into the target position calculation. As a result, the difference between the derived target positions was found to be less than 60 mm. Considering that the diameter of a standard dinner plate is approximately 250 mm (10 inches), such deviations are within an acceptable margin of error. An analysis of the movement and EMG data collected during this experiment revealed a robust correlation between the intermediate position and the EMG signals from the deltoid-anterior and pectoralis major (clavicular head) muscles. Notably, as the participants approached the intermediate position, there was a marked peak in the EMG-RMS signals of either muscle, followed by its inaugural negative rate of change. This pattern was observed for all test participants, demonstrating the efficacy of using EMG-RMS signals from the deltoid-anterior and pectoralis major (clavicular head) muscles as indicators of the user's arrival at the intermediate position. Furthermore, the inferred intermediate position was combined with the initial position to estimate the target position of the users.

To determine the reference posture based on the real-time utensil location, a three-layer neural network regressor, as illustrated in Table 3, was employed in this study. The neural network regressor was designed to accept three input features: utensil trajectory data (along the x-, y-, and z-axes), the index of the user's target position (from 1 to 9) and the type of utensil being used (fork, chopsticks, or spoon). These inputs were transmitted to a hidden layer, which included 40 neurons. The neurons in this layer use the hyperbolic tangent function for activation to introduce nonlinearities, while the output layer had a linear activation function to estimate the reference utensil posture [61]. The network employed error backpropagation learning algorithm for training, with weights initially set at random and optimized during training

TABLE 3. Structure and hyperparameters of the neural network regressor.

Layer	Input layer	Hidden layer	Output layer
Neuron count	5	40	3
Activation function	-	Hyperbolic tangent	Linear
Error function	Mean squared error loss function		
Learning algorithm	Error backpropagation		
Learning rate	0.0001		
Dropout rate	0.3		

TABLE 4. R-squared statistics of the neural network regressor used in the X-Y, Z-X, and Z-X directions.

Reference utensil posture	R^2	RMSE
$\theta_{ref,xy}$	0.93	1.88°
$\theta_{ref,xz}$	0.88	1.69°
$\theta_{ref,yz}$	0.97	1.54°

TABLE 5. Error between the real average utensil posture of three subjects and that estimated by the neural network regressor.

Error	$\theta_{ref,xy}$	$\theta_{ref,xz}$	$\theta_{ref,yz}$
Mean	3.55°	2.87°	2.37°
Max	13.18°	11.90°	8.58°

to minimize prediction errors [62]. The mean squared error loss function quantified the discrepancy between the predictions and actual outputs, and the learning rate was set at 0.0001 to control weight adjustments [63], [64]. To prevent overfitting, a dropout technique randomly disabled 30% of the neurons per layer in each iteration, enhancing the generalizability [65]. Additionally, the network used normalization to enhance training stability and efficiency, and denormalization to interpret outputs at their original data scale, optimizing performance [66]. To ensure that the model captures broad behavioral patterns and considers the potential variations between individual subjects, the average data from three participants were utilized in the experiments. The averaged data were divided into three sets: two sets were used for training, and the remaining set was reserved for testing.

The accuracy of the neural network regressor was verified by comparing the utensil posture estimated by the trained neural network to the actual posture in the x-y, x-z, and y-z directions. The R^2 statistic was used to evaluate the reliability of the modeling results. The R^2 statistic is defined as follows:

$$R^2 = 1 - \frac{\sum_{i=1}^{n} \left(y_i - \hat{y}_i\right)^2}{\sum_{i=1}^{n} \left(y_i - \bar{y}_i\right)^2} \tag{24}$$

where y_i represents the actual utensil posture, $\hat{y}_i$ represents the estimated posture, and $\bar{y}$ is the mean of the actual utensil posture. R^2 values range between 0 and 1. A higher R^2 value typically indicates that the trained model fits the data better. The R^2 values for the three utensil postures, $\boldsymbol{\theta_{ref,xy}}$, $\boldsymbol{\theta_{ref,xz}}$ and $\boldsymbol{\theta_{ref,yz}}$, are shown in Table 4, and the values are 0.93, 0.88, and 0.97, respectively. Furthermore, the root mean square error (RMSE) was used to validate the estimation results. The RMSE values for the estimated utensil postures in the x-y, x-z, and y-z directions were 1.88°, 1.69°, and 1.54° respectively.

The maximum absolute errors between the estimated utensil posture and the actual posture in the x-y, x-z, and y-z directions are 13.18°, 11.90° and 8.58°, respectively. The experimental results confirm the effectiveness of using the neural network regressor to identify the reference utensil

posture accurately. Given the current position of the utensil, this regressor can predict the reference utensil posture.

B. EXPERIMENT-2

The results of experiment-2 are presented in Figs. 9-11, which correspond to trials A, B and C, respectively. In these trials, by generating two interconnected virtual tunnels in space, the utensil trajectory and/or posture were modified when they were found to be inappropriate. The effectiveness of this method is determined by its ability to detect deviations and autonomously correct inappropriate utensil trajectories/postures that exceed the boundaries of the virtual tunnels, thereby restoring the user's motion to an appropriate state. In Fig. 9-11(a), the green region represents the extent of the virtual tunnel formed for the utensil trajectory, with the external boundary indicated by the dot-dashed green lines. The orange solid line represents the shortest distance, ***sDist***, from the utensil tip to the reference trajectory. The black dot-dashed, dotted, and dashed lines represent the deviations $\boldsymbol{sDist_x}$, $\boldsymbol{sDist_y}$, and $\boldsymbol{sDist_z}$ in the x (i.e., forward/backward), y (i.e., left/right), and z (i.e., up/down) directions, respectively. In Fig. 9-11(b), the blue dot-dashed line, yellow dot-dotted line, and gray dashed line illustrate the modification forces in the x, y, and z directions, respectively. In Fig. 9-11(c), the green region represents the virtual tunnel formed for the utensil posture, with a similar dot-dashed green boundary. The solid blue, yellow, and gray lines represent the deviations $\boldsymbol{\theta_{gap}}$ between the actual and reference utensil postures in the z-y ($\boldsymbol{\theta_{gap,zy}}$), z-x ($\boldsymbol{\theta_{gap,zx}}$), and x-y ($\boldsymbol{\theta_{gap,xy}}$) directions, respectively. If the deviations exceed the allowable range, posture modification torques are exerted in the corresponding directions. In Fig. 9-11(d), the torques in the z-y, z-x, and x-y directions are depicted by the blue dot-dashed, yellow dot-dotted, and gray dashed lines, respectively. Since the virtual tunnels are generated after the target position is determined, there is no initial phase evaluation or modification of the motion. Evaluation and adjustments to correct any improper utensil trajectories and/or postures become possible after the target position has been assessed and tunnels have formed, as depicted in the results (Figs. 9-11).

Fig. 9 presents the experimental results for trial A, in which an inappropriate utensil trajectory was used for the motion. The exoskeleton determines the deviation ***sDist***, as illustrated in Fig. 9(a), to determine if and in which directions the motion should be modified to align the trajectory toward the target position. The evaluation results show that when ***sDist*** surpassed the tunnel boundary, $\boldsymbol{sDist_x}$ exceeded the constraint in the x direction. Hence, a motion modification force was progressively applied by the exoskeleton in the x direction, and its magnitude increased with the deviation ***sDist*** and peaked when the deviation crossed the external boundary. Aided by this force, the tip position crossed the outer boundary, at which point the modification force decreased until the tip position re-entered the allowable range; then, the modification force was stopped. The trajectory was subsequently adjusted within the virtual tunnel. Since the necessary

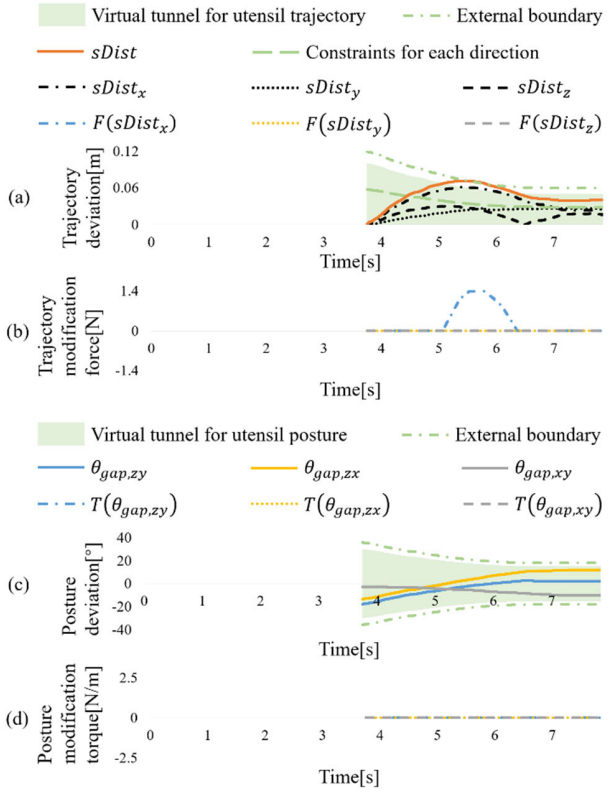

FIGURE 9. Experiment results for trial A. (a) Trajectory deviation. (b) Trajectory modification force. (c) Posture deviation. (d) Posture modification torque.

condition in the y and z directions are not satisfied, the motion in those directions was not modified. During the entire trial, the utensil posture consistently remained within the acceptable limits, so no posture modification torque was applied (Fig. 9(c) and 9(d)). The trial A results confirmed that trajectory modification for an impropriate utensil trajectory can be realized as expected.

Fig. 10 shows the experimental results for trial B, in which the motion was executed with an inappropriate utensil posture. In this trial, no motion modification force was applied, as the utensil trajectory consistently remained within the virtual tunnel throughout the entire trial (Fig. 10(a) and 10(b)). As illustrated in Fig. 10(c) and 10(d), upon the initial generation of the virtual tunnels, the deviation angles $\boldsymbol{\theta_{gap,zy}}$ and $\boldsymbol{\theta_{gap,xy}}$ surpassed the tolerance angle of the posture virtual tunnel in the z-y and x-y directions. This indicates that the postures in these directions were unsuitable, with the posture in the x-y direction deviating beyond the external boundary. To correct the posture, modification torques were applied to guide the posture toward the virtual tunnel. As the posture in each direction returned to the virtual tunnel, the applied modification torques were gradually reduced and finally stopped. The posture in the z-x direction did not meet the necessary condition for adjustment, so no modification torque was applied in that direction. The outcomes of trial B

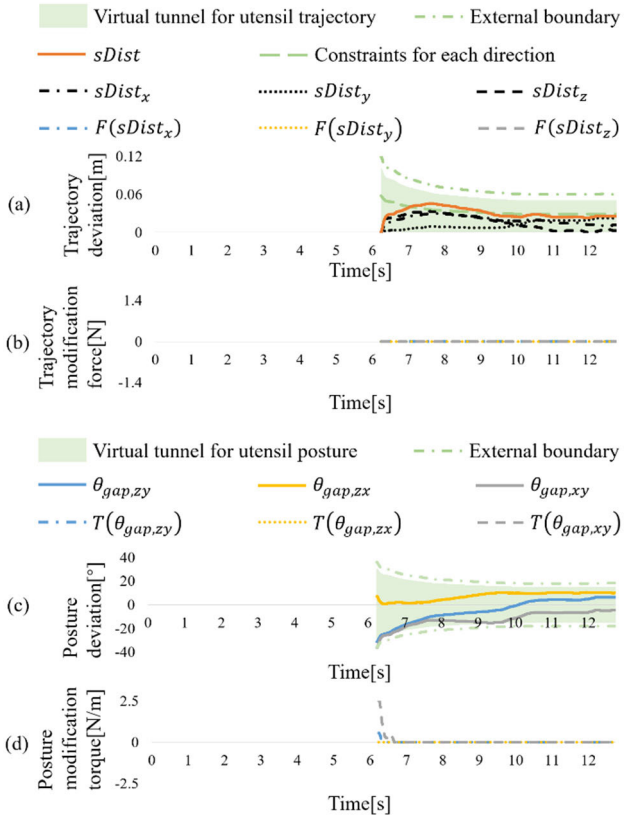

FIGURE 10. Experiment results for trial B. (a) Trajectory deviation. (b) Trajectory modification force. (c) Posture deviation. (d) Posture modification torque.

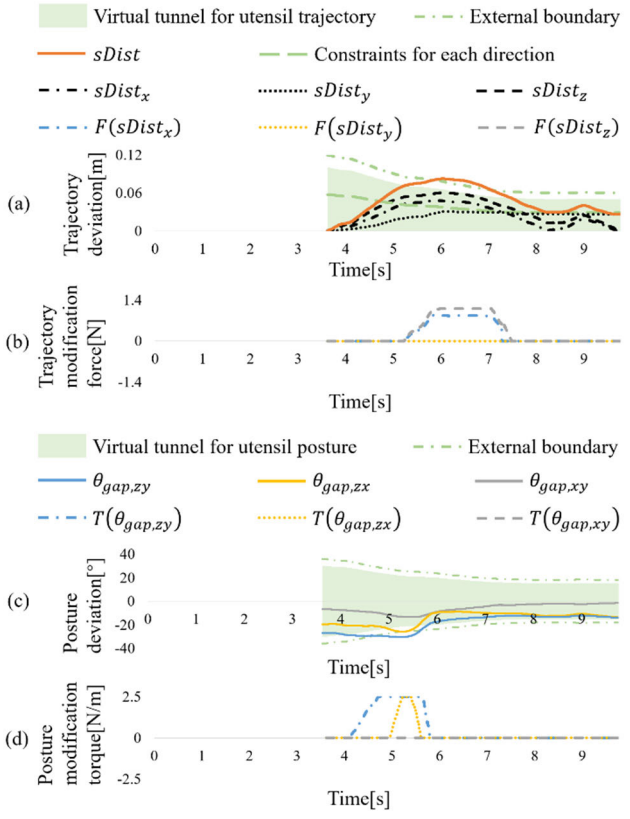

FIGURE 11. Experiment results for trial C. (a) Trajectory deviation. (b) Trajectory modification force. (c) Posture deviation. (d) Posture modification torque.

confirmed that modifications for unsuitable utensil postures can be effectively executed, as expected.

Fig. 11 illustrates the results of trial C, during which both incorrect utensil trajectory and posture were executed. As shown in Fig. 11(a), after ***sDist*** crossed the tunnel boundary, $\boldsymbol{sDist_x}$ and $\boldsymbol{sDist_z}$ exceeded their respective constraints in the x and z directions. Consequently, the exoskeleton deployed modification forces in these directions that were proportional to the magnitude of the deviation. The forces increased as ***sDist*** increased and reached their maximum values when the deviations crossed the outer boundary. This force guided the tip back toward the boundary and decreased when the tip was within the allowed range; thus, the trajectory was readjusted toward the virtual tunnel. No modifications were made in the y direction as the condition was not violated in this direction. Figs. 11(c) and 11(d) show the posture deviations $\boldsymbol{\theta_{gap,zy}}$ and $\boldsymbol{\theta_{gap,zx}}$ in the z-y and z-x directions, respectively. These deviations exceed the virtual tunnel, indicating inappropriate postures in these directions. To correct these postures, modification torques were introduced to guide the posture toward the virtual tunnel. As the posture in each direction returned to the virtual tunnel, the applied modification torques were gradually reduced and finally stopped. The posture in the x-y direction did not meet the necessary condition for adjustment, so no modification torque was applied in that direction. The results of trial C confirmed that trajectory modification and posture modification for impropriate utensil trajectories/postures can be realized, as expected.

Based on these experimental results, the virtual tunnel generation mechanism for the utensil trajectory and utensil posture during meal activities can be effectively executed by applying the proposed perception assist method. This allows for real-time identification and modification of inappropriate utensil trajectories and/or postures, enhancing the user's performance in meal activities. Other investigations have shown that, in both perception assist [15], [16], [17], [18], [19], [20] and rehabilitation [49], [50], [51], establishing a virtual space such as a virtual tunnel is beneficial for evaluating the rationality of user motion and modifying unreasonable motions. In conclusion, the proposed method can effectively assist users with meal activities.

V. CONCLUSION AND FUTURE WORK

In this study, a perception assist method integrated with an upper limb power assist exoskeleton robot is proposed, aimed at aiding individuals with perception impairments in performing meal activities. The proposed method includes two main components: first, the user's target position is determined based on the utensil trajectory and the user's shoulder EMG signals (deltoid-anterior and pectoralis major

(clavicular head) muscles); then, inappropriate utensil trajectories and/or postures are identified and modified through two spatially related virtual tunnels. To validate the effectiveness of this method, two experiments were conducted. The results demonstrated that the shoulder EMG signals could be used to effectively identify intermediate positions in the utensil trajectory during motion, enabling accurate inference of the user's target position. Additionally, the neural network regressor successfully mapped the spatial relationship between the reference utensil trajectory and the utensil posture. Importantly, the proposed technique could correct inappropriate utensil trajectories and postures in real time with the assistance of an upper limb power assist exoskeleton robot. The proposed method is assumed to be universally applicable across a variety of tasks that require coordinating the position and posture of a utensil. This includes tasks similar to meal activities, which involve nonlinear motion trajectories where the user should initially raise the utensil before lowering it toward the target position. Although the proposed target position prediction method using EMG signals is applicable to such movements, it might not be applicable to other types of reaching movements. While this study involved young, healthy individuals, future research aims to include participants from a broader range of ages and physical conditions to comprehensively evaluate the influence of these factors.

REFERENCES

[1] S. Ogura and M. M. Jakovljevic, "Global population aging-health care, social and economic consequences," *Frontiers Public Health*, vol. 6, Nov. 2018.

[2] C.-J. Yang, J.-F. Zhang, Y. Chen, Y.-M. Dong, and Y. Zhang, "A review of exoskeleton-type systems and their key technologies," *Proc. Inst. Mech. Eng, C, J. Mech. Eng. Sci.*, vol. 222, no. 8, pp. 1599–1612, Aug. 2008.

[3] R. A. R. C. Gopura, D. S. V. Bandara, K. Kiguchi, and G. K. I. Mann, "Developments in hardware systems of active upper-limb exoskeleton robots: A review," *Robot. Auto. Syst.*, vol. 75, pp. 203–220, Jan. 2016.

[4] K. Kiguchi and Y. Hayashi, "An EMG-based control for an upper-limb power-assist exoskeleton robot," *IEEE Trans. Syst. Man, Cybern., B, Cybern.*, vol. 42, no. 4, pp. 1064–1071, Aug. 2012.

[5] J. Huang, W. Huo, W. Xu, S. Mohammed, and Y. Amirat, "Control of upper-limb power-assist exoskeleton using a human-robot interface based on motion intention recognition," *IEEE Trans. Autom. Sci. Eng.*, vol. 12, no. 4, pp. 1257–1270, Oct. 2015.

[6] Z. Li, B. Wang, F. Sun, C. Yang, Q. Xie, and W. Zhang, "SEMG-based joint force control for an upper-limb power-assist exoskeleton robot," *IEEE J. Biomed. Health Informat.*, vol. 18, no. 3, pp. 1043–1050, May 2014.

[7] Z. Tang, K. Zhang, S. Sun, Z. Gao, L. Zhang, and Z. Yang, "An upper-limb power-assist exoskeleton using proportional myoelectric control," *Sensors*, vol. 14, no. 4, pp. 6677–6694, Apr. 2014.

[8] D. Ao, R. Song, and J. Gao, "Movement performance of human–robot cooperation control based on EMG-driven hill-type and proportional models for an ankle power-assist exoskeleton robot," *IEEE Trans. Neural Syst. Rehabil. Eng.*, vol. 25, no. 8, pp. 1125–1134, Aug. 2017.

[9] P. B. Baltes and U. Lindenberger, "Emergence of a powerful connection between sensory and cognitive functions across the adult life span: A new window to the study of cognitive aging?" *Psychol. Aging*, vol. 12, no. 1, pp. 12–21, 1997.

[10] I. Ulrich and J. Borenstein, "The GuideCane-applying mobile robot technologies to assist the visually impaired," *IEEE Trans. Syst., Man, Cybern. A, Syst. Humans*, vol. 31, no. 2, pp. 131–136, Mar. 2001.

[11] V. Kulyukin, C. Gharpure, J. Nicholson, and S. Pavithran, "RFID in robot-assisted indoor navigation for the visually impaired," in *Proc. IEEE/RSJ Int. Conf. Intell. Robots Syst. (IROS)*, vol. 2, Jun. 2004, pp. 1979–1984.

[12] D. Ni, A. Song, L. Tian, X. Xu, and D. Chen, "A walking assistant robotic system for the visually impaired based on computer vision and tactile perception," *Int. J. Social Robot.*, vol. 7, no. 5, pp. 617–628, Nov. 2015.

[13] S.-Y. Jiang, C.-Y. Lin, K.-T. Huang, and K.-T. Song, "Shared control design of a walking-assistant robot," *IEEE Trans. Control Syst. Technol.*, vol. 25, no. 6, pp. 2143–2150, Nov. 2017.

[14] M. Geravand, C. Werner, K. Hauer, and A. Peer, "An integrated decision making approach for adaptive shared control of mobility assistance robots," *Int. J. Social Robot.*, vol. 8, no. 5, pp. 631–648, Nov. 2016.

[15] Y. Hirata, A. Hara, and K. Kosuge, "Motion control of passive-type walking support system based on environment information," in *Proc. IEEE Int. Conf. Robot. Autom.*, Barcelona, Spain, Apr. 2005, pp. 2921–2926.

[16] D.-X. Liu, J. Xu, C. Chen, X. Long, D. Tao, and X. Wu, "Vision-assisted autonomous lower-limb exoskeleton robot," *IEEE Trans. Syst. Man, Cybern. Syst.*, vol. 51, no. 6, pp. 3759–3770, Jun. 2021.

[17] B. Zhong, R. L. d. Silva, M. Li, H. Huang, and E. Lobaton, "Environmental context prediction for lower limb prostheses with uncertainty quantification," *IEEE Trans. Autom. Sci. Eng.*, vol. 18, no. 2, pp. 458–470, Apr. 2021.

[18] Y. Hayashi and K. Kiguchi, "A lower-limb power-assist robot with perception-assist," in *Proc. IEEE Int. Conf. Rehabil. Robot.*, Zurich, Switzerland, Jun. 2011, pp. 1–6.

[19] K. Kiguchi and Y. Yokomine, "Perception-assist with a lower-limb power-assist robot for sitting motion," in *Proc. IEEE Int. Conf. Syst., Man, Cybern.*, Hong Kong, Oct. 2015, pp. 2390–2394.

[20] Y. Hayashi and K. Kiguchi, "Stairs-ascending/descending assist for a lower-limb power-assist robot considering ZMP," in *Proc. IEEE/RSJ Int. Conf. Intell. Robots Syst.*, San Francisco, CA, USA, Sep. 2011, pp. 1755–1760.

[21] K. Kiguchi, M. Liyanage, and Y. Kose, "Perception-assist with an active stereo camera for an upper-limb power-assist exoskeleton," *J. Robot. Mechatronics*, vol. 21, no. 5, pp. 614–620, Oct. 2009.

[22] K. Kiguchi, Y. Kose, and Y. Hayashi, "An upper-limb power-assist exoskeleton robot with task-oriented perception-assist," in *Proc. 3rd IEEE RAS EMBS Int. Conf. Biomed. Robot. Biomechatronics*, Sep. 2010, pp. 88–93.

[23] Y. Hou and K. Kiguchi, "Virtual tunnel generation algorithm for perception-assist with an upper-limb exoskeleton robot," in *Proc. IEEE Int. Conf. Cyborg Bionic Syst. (CBS)*, Shenzhen, China, Oct. 2018, pp. 204–209.

[24] K. G. M. Chathuramali and K. Kiguchi, "Real-time detection of the interaction between an upper-limb power-assist robot user and another person for perception-assist," *Cognit. Syst. Res.*, vol. 61, pp. 53–63, Jun. 2020.

[25] G. Kwakkel, B. J. Kollen, and H. I. Krebs, "Effects of robot-assisted therapy on upper limb recovery after stroke: A systematic review," *Neurorehabilitation Neural Repair*, vol. 22, no. 2, pp. 111–121, Mar. 2008.

[26] P. Maciejasz, J. Eschweiler, K. Gerlach-Hahn, A. Jansen-Troy, and S. Leonhardt, "A survey on robotic devices for upper limb rehabilitation," *J. NeuroEng. Rehabil.*, vol. 11, no. 1, pp. 1–29, Dec. 2014.

[27] G. Zeilig, H. Weingarden, M. Zwecker, I. Dudkiewicz, A. Bloch, and A. Esquenazi, "Safety and tolerance of the ReWalk exoskeleton suit for ambulation by people with complete spinal cord injury: A pilot study," *J. Spinal Cord Med.*, vol. 35, no. 2, pp. 96–101, Mar. 2012.

[28] S. A. Kolakowsky-Hayner, "Safety and feasibility of using the EksoTM bionic exoskeleton to aid ambulation after spinal cord injury," *J. Spine*, vol. 4, p. 3, Jan. 2013.

[29] T. Gurriet, S. Finet, G. Boeris, A. Duburcq, A. Hereid, O. Harib, M. Masselin, J. Grizzle, and A. D. Ames, "Towards restoring locomotion for paraplegics: Realizing dynamically stable walking on exoskeletons," in *Proc. IEEE Int. Conf. Robot. Autom. (ICRA)*, May 2018, pp. 2804–2811.

[30] H. C. Ravichandar, D. Trombetta, and A. P. Dani, "Human intention-driven learning control for trajectory synchronization in human-robot collaborative tasks," *IFAC-PapersOnLine*, vol. 51, no. 34, pp. 1–7, 2019.

[31] H. Liu and L. Wang, "Human motion prediction for human-robot collaboration," *J. Manuf. Syst.*, vol. 44, pp. 287–294, Jul. 2017.

[32] Y. Huo, X. Li, X. Zhang, and D. Sun, "Intention-driven variable impedance control for physical human-robot interaction," in *Proc. IEEE/ASME Int. Conf. Adv. Intell. Mechatronics (AIM)*, Delft, The Netherlands, Jul. 2021, pp. 1220–1225.

[33] A. P. Dani, I. Salehi, G. Rotithor, D. Trombetta, and H. Ravichandar, "Human-in-the-loop robot control for human-robot collaboration: Human intention estimation and safe trajectory tracking control for collaborative tasks," *IEEE Control Syst. Mag.*, vol. 40, no. 6, pp. 29–56, Dec. 2020.

[34] M. Awais, M. Y. Saeed, M. S. A. Malik, M. Younas, and S. R. I. Asif, "Intention based comparative analysis of human-robot interaction," *IEEE Access*, vol. 8, pp. 205821–205835, 2020.
[35] Q. Li, Z. Zhang, Y. You, Y. Mu, and C. Feng, "Data driven models for human motion prediction in human-robot collaboration," *IEEE Access*, vol. 8, pp. 227690–227702, 2020.
[36] Y. Li and S. S. Ge, "Human–robot collaboration based on motion intention estimation," *IEEE/ASME Trans. Mechatronics*, vol. 19, no. 3, pp. 1007–1014, Jun. 2014.
[37] R. Stiefelhagen, C. Fogen, P. Gieselmann, H. Holzapfel, K. Nickel, and A. Waibel, "Natural human-robot interaction using speech, head pose and gestures," in *Proc. IEEE/RSJ Int. Conf. Intell. Robots Syst. (IROS)*, vol. 3, Sendai, Japan, Sep. 2004, pp. 2422–2427.
[38] A. Shafti, P. Orlov, and A. A. Faisal, "Gaze-based, context-aware robotic system for assisted reaching and grasping," in *Proc. Int. Conf. Robot. Autom. (ICRA)*, Montreal, QC, Canada, May 2019, pp. 863–869.
[39] A. Frisoli, C. Loconsole, D. Leonardis, F. Banno, M. Barsotti, C. Chisari, and M. Bergamasco, "A new gaze-BCI-driven control of an upper limb exoskeleton for rehabilitation in real-world tasks," *IEEE Trans. Syst. Man, Cybern., C, Appl. Rev.*, vol. 42, no. 6, pp. 1169–1179, Nov. 2012.
[40] P. Schydlo, M. Rakovic, L. Jamone, and J. Santos-Victor, "Anticipation in human-robot cooperation: A recurrent neural network approach for multiple action sequences prediction," in *Proc. IEEE Int. Conf. Robot. Autom. (ICRA)*, May 2018, pp. 5909–5914.
[41] J. Kuhn, J. Ringwald, M. Schappler, L. Johannsmeier, and S. Haddadin, "Towards semi-autonomous and soft-robotics enabled upper-limb exo-prosthetics: First concepts and robot-based emulation prototype," in *Proc. Int. Conf. Robot. Autom. (ICRA)*, Montreal, QC, Canada, May 2019, pp. 9180–9186.
[42] L. Bi, S. Xia, and W. Fei, "Hierarchical decoding model of upper limb movement intention from EEG signals based on attention state estimation," *IEEE Trans. Neural Syst. Rehabil. Eng.*, vol. 29, pp. 2008–2016, 2021.
[43] Y. Feng, H. Wang, L. Vladareanu, Z. Chen, and D. Jin, "New motion intention acquisition method of lower limb rehabilitation robot based on static torque sensors," *Sensors*, vol. 19, no. 15, p. 3439, Aug. 2019.
[44] Y. Zhuang, S. Yao, C. Ma, and R. Song, "Admittance control based on EMG-driven musculoskeletal model improves the human–robot synchronization," *IEEE Trans. Ind. Informat.*, vol. 15, no. 2, pp. 1211–1218, Feb. 2019.
[45] M. Martins, A. Frizera-Neto, C. Santos, and R. C. Ruiz, "Smart Walker control through the inference of the user's command intentions," in *Proc. Int. Conf. Inform. Control, Autom. Robot.*, 2012, pp. 458–463.
[46] D. Novak, X. Omlin, R. Leins-Hess, and R. Riener, "Predicting targets of human reaching motions using different sensing technologies," *IEEE Trans. Biomed. Eng.*, vol. 60, no. 9, pp. 2645–2654, Sep. 2013.
[47] B. T. Carter and S. G. Luke, "Best practices in eye tracking research," *Int. J. Psychophysiol.*, vol. 155, pp. 49–62, Sep. 2020.
[48] G. Chen, J. Ye, Q. Liu, L. Duan, W. Li, Z. Wu, and C. Wang, "Adaptive control strategy for gait rehabilitation robot to assist-when-needed," in *Proc. IEEE Int. Conf. Real-time Comput. Robot. (RCAR)*, Kandima, Maldives, Aug. 2018, pp. 538–543.
[49] A. Duschau-Wicke, J. von Zitzewitz, A. Caprez, L. Lunenburger, and R. Riener, "Path control: A method for patient-cooperative robot-aided gait rehabilitation," *IEEE Trans. Neural Syst. Rehabil. Eng.*, vol. 18, no. 1, pp. 38–48, Feb. 2010.
[50] H. I. Krebs, "Rehabilitation robotics: Performance-based progressive robot-assisted therapy," *Auto. Robots*, vol. 15, pp. 7–20, Jul. 2003.
[51] L. L. Cai, A. J. Fong, C. K. Otoshi, Y. Liang, J. W. Burdick, R. R. Roy, and V. R. Edgerton, "Implications of assist-as-needed robotic step training after a complete spinal cord injury on intrinsic strategies of motor learning," *J. Neurosci.*, vol. 26, no. 41, pp. 10564–10568, Oct. 2006.
[52] S. K. Banala, S. H. Kim, S. K. Agrawal, and J. P. Scholz, "Robot assisted gait training with active leg exoskeleton (ALEX)," *IEEE Trans. Neural Syst. Rehabil. Eng.*, vol. 17, no. 1, pp. 2–8, Feb. 2009.
[53] U. Keller, G. Rauter, and R. Riener, "Assist-as-needed path control for the PASCAL rehabilitation robot," in *Proc. IEEE 13th Int. Conf. Rehabil. Robot. (ICORR)*, Seattle, WA, USA, Jun. 2013, pp. 1–7.
[54] I. Kang, P. Kunapuli, and A. J. Young, "Real-time neural network-based gait phase estimation using a robotic hip exoskeleton," *IEEE Trans. Med. Robot. Bionics*, vol. 2, no. 1, pp. 28–37, Feb. 2020.
[55] D. Xu, X. Liu, and Q. Wang, "Knee exoskeleton assistive torque control based on real-time gait event detection," *IEEE Trans. Med. Robot. Bionics*, vol. 1, no. 3, pp. 158–168, Aug. 2019.
[56] Y. Miura, S. Nagasaki, and H. Fukushima, "The reach movement that is used to eat," *J. Kansai Phys. therapy*, vol. 15, pp. 7–11, Jan. 2015.
[57] M. E. Paton and J. M. M. Brown, "An electromyographic analysis of functional differentiation in human pectoralis major muscle," *J. Electromyogr. Kinesiol.*, vol. 4, no. 3, pp. 161–169, Jan. 1994.
[58] R. Sugahara, "Electromyographic study on shoulder movements," *Jpn. J. Rehabil. Med.*, vol. 11, no. 1, pp. 41–53, 1974.
[59] D. Wattanaprakornkul, M. Halaki, C. Boettcher, I. Cathers, and K. A. Ginn, "A comprehensive analysis of muscle recruitment patterns during shoulder flexion: An electromyographic study," *Clin. Anatomy*, vol. 24, no. 5, pp. 619–626, Jul. 2011.
[60] K. Kiguchi, M. Liyanage, and Y. Kose, "Intelligent perception assist with optimum force vector modification for an upper-limb power-assist exoskeleton," in *Proc. 2nd IEEE RAS EMBS Int. Conf. Biomed. Robot. Biomechatronics*, Scottsdale, AZ, USA, Oct. 2008, pp. 175–180.
[61] C. Nwankpa, W. Ijomah, A. Gachagan, and S. Marshall, "Activation functions: Comparison of trends in practice and research for deep learning," 2018, *arXiv:1811.03378*.
[62] R. Rojas, "The backpropagation algorithm," in *Neural Networks: A Systematic Introduction*. Berlin, Germany: Springer, 1996, pp. 149–182.
[63] A. R. Barron, "Approximation and estimation bounds for artificial neural networks," *Mach. Learn.*, vol. 14, no. 1, pp. 115–133, Jan. 1994.
[64] A. Senior, G. Heigold, M. Ranzato, and K. Yang, "An empirical study of learning rates in deep neural networks for speech recognition," in *Proc. IEEE Int. Conf. Acoust., Speech Signal Process.*, Vancouver, BC, Canada, May 2013, pp. 6724–6728.
[65] N. Srivastava, G. Hinton, A. Krizhevsky, I. Sutskever, and R. Salakhutdinov, "Dropout: A simple way to prevent neural networks from overfitting," *J. Mach. Learn. Res.*, vol. 15, no. 1, pp. 1929–1958, Jan. 2014.
[66] P. J. M. Ali and R. H. Faraj, "Data normalization and standardization: A technical report," *Mach. Learn. Tech. Rep.*, vol. 1, no. 1, pp. 1–6, 2014.

YUE HOU (Student Member, IEEE) received the B.E. degree from Tianjin University of Science and Technology, Tianjin, China, in 2015, and the M.E. degree in mechanical engineering from Kyushu University, Fukuoka, Japan, in 2019, where she is currently pursuing the D.E. degree. Her research interests include human-assist robots and human–machine interaction.

KAZUO KIGUCHI (Senior Member, IEEE) received the B.E. degree from Niigata University, Niigata, Japan, in 1986, the M.A.Sc. degree from the University of Ottawa, Ottawa, Canada, in 1993, and the D.E. degree from Nagoya University, Nagoya, Japan, in 1997.

He was with Mazda Motor Corporation, from 1986 to 1989, and MHI Aerospace Systems Corporation, from 1989 to 1991. From 1994 and 1999, he was with Niigata College of Technology, Niigata. He was with the Graduate School of Science and Engineering, Saga University, Japan, from 1999 and 2012. He is currently a Professor with the Department of Mechanical Engineering, Faculty of Engineering, Kyushu University, Japan. His research interests include bio robotics, human-assist robots, rehabilitation robots, and the application of robotics in medicine. He is a Senior Member of the IEEE (Robotics and Automation, Systems, Man, and Cybernetics, Computational Intelligence, and Engineering in Medicine and Biology Societies) and a member of the Robotics Society of Japan, Japan Society of Computer-Aided Surgery, the Society of Biomechanisms Japan, and the Japanese Society for Medical and Biological Engineering. He is a fellow of Japan Society of Mechanical Engineers (JSME) and the Society of Instrument and Control Engineers (SICE). He received the JSME Funai Award, the JSME Medal for Outstanding Paper, and the JSME Medal for Distinguished Engineers, Lifetime Achievement Award at WAC2014.